

ENHANCEMENT OF GROWTH IN MAIZE BY BIOGENIC- SYNTHESIZED MgO NANOPARTICLES

Jayarambabu N¹, Siva Kumari B¹, Venkateswara Rao K², Prabhu YT²

¹Department of Botany, Andhra Loyola College, Vijayawada, Andhra Pradesh, India

²Centre for Nano Science and Technology, Institute of Science and Technology, Jawaharlal Nehru Technological University Hyderabad, Kukatpally, Hyderabad, Telangana-500085, India

Article History: Received 02nd April 2016; Accepted 27th June 2016; Published 07th July 2016

The magnesium oxide nanoparticles (MgO NPs) were synthesized using aqueous leaf extracts of (Betel) by bio combustion method. The synthesized magnesium oxide nanoparticles were characterized by XRD, FTIR, TG/DTA, PSA and SEM. The seeds treated with synthesized MgO NPs showed better germination but the seedling growth of tested species was affected when exposed to concentrations of MgO NPs. In this experiment mainly focused physical characteristics of the maize plants like, germination percentage (GP), germination index (GI), vigor seedling index (VSI), relative seed germination (RSG), relative root growth (RRG), Biomass, Root length and shoot length. Magnesium oxide nanoparticles may hold significant applications in agriculture and gardening by selectively inhibiting harmful fungi and bacteria presents on seeds and could provide as an alternative source of fertilizer that may improve sustainable agriculture. The chlorophyll test was carryout after 20 days maize plants, the low concentration MgO NPs treated maize plant shown chlorophyll content increase when compare to other treatments and control.

Keywords: Betel leaf extract; MgO nanoparticles; Maize seeds; Germination; Growth parameters; Chlorophyll.

INTRODUCTION

Nanotechnology application is now widely distributed throughout life, and especially in agricultural systems. Nanoparticles, because of their physicochemical characteristics, are among the potential candidates for modulating the redox status and changing the seed germination, growth, performance, and quality of plants (Adams, 2006). The numerous studies have reported the effects of NPs on seed germination and crops improvement. However, most of the experiments have been done under controlled conditions. Both carbon based ENPs and metal and metal-oxide ENPs have been the subject of these studies. Such carbon nanomaterials (such as Single-walled carbon nanotubes (SWCNTs), multi-walled carbon nanotube (MWCNTs), carbon bucky balls, etc.) are finding application in seed germination and agriculture and food packaging. This has raised questions regarding the safety of using such ENPs in agriculture. Conflicting evidences are available regarding the effect of ENPs on crops (Aoshima, 2009). Studies indicate that carbon nanotubes (CNTs) penetrated tomato seeds and dramatically enhanced their germination percentage and growth parameters (Aruoja, 2009). They suggested that the CNTs were able to easily penetrate the thick seed coat and support water uptake inside seeds, a process which can enhance seed germination and growth of tomato seedlings. (Brar, 2010) Few other studies also support the positive effects of suspensions

of MWCNTs on seed germination and root growth of six different crop species [radish (*Raphanus sativus*), rape (*Brassica napus*), rye grass (*Lolium perenne*), lettuce (*Lactuca sativa*), corn (*Zea mays*) and cucumber (*Cucumis sativus*)]. TiO₂ NPs have been found to improve light absorbance and promote the activity of Rubisco activase thus accelerating spinach growth (Canas, 2008). TiO₂ NP (anatase) also improved plant growth by enhanced nitrogen metabolism (Colvin, 2003) that promotes the absorption of nitrate in spinach an accelerating conversion of inorganic nitrogen into organic nitrogen, thereby increasing efficiency of plant fresh weights and dry weights (DeRosa, 2010). In this experiment studies on maize growth parameters, germination percentage and chlorophyll content treated with biological synthesized MgO nanoparticles.

MATERIALS AND METHODS

Materials used

Magnesium acetate, betel leaf extract are used as reducing agent and stabilizing agent.

Green synthesis method

In this green synthesis method MgO nanoparticles are prepared. It is simple, fast and environment friendly method. 0.05 M of Magnesium acetate were used as the precursor material and mixed with 50 ml distilled water under vigorous stir for 30 minutes. For this solution 25 ml

Table 1: Characteristics of the experimental soil.

Parameter	Quantity
Sand (%)	82.1
Slit (%)	7.9
Clay (%)	6.5
pH	7.9
Organic matter (%)	0.39
Total N (mg.kg ⁻¹)	432
Total P (mg.kg ⁻¹)	633
Total K (mg.kg ⁻¹)	632

of prepared betel leaf extract used as a reducing agent and was added under stirring for 30 min. Then the mixed solution was placed on hot plate for 4 hours at 110°C then collected sample crushed into powder using mortar and pestle. The dried precursor then was calcinated at 400°C.

Nanoparticles suspensions

The metal oxide nanoparticles were suspended directly in Millipore water and dispersed by ultrasonic vibration (250W, 20 kHz) for 30 minutes using the Ultrasonic. The nanoparticles concentration of 50, 100 and 150 mg.L⁻¹ suspensions were prepared (Table 1).

Seedling exposure

The seeds were checked for their viability by suspending them in double distilled water. The seeds which are settled to the bottom were selected for further study. The seeds were rinsed in double distilled water thrice and then surface sterilization of seeds was done. The biological synthesized MgO nanoparticles were sonicated for 30 minutes. The nanoparticles, then add the sterilized seeds in prepared nanoparticle suspensions (0.0, 50, 100 150 mg/L⁻¹) using a sonicator instrument. The soaked seeds were put in prepared pots and observe of the growth.

Seed germination percentage

The counts were taken as per the ISTA rules (1993) and expressed in percentage.

The seed germination rate (RSG) and relative root growth (RRG) were calculated using the equation (1) and (2). The germination index (GI) was calculated using equation (3)

$$\text{Relative Seed Rate Germination Rate} = \left(\frac{S_c}{S_s} \right) 100 \quad (1)$$

$$\text{Relative Root Growth} = \left(\frac{R_s}{R_c} \right) 100 \quad (2)$$

$$\text{Germination Index} = \left(\frac{RSG}{RRG} \right) 100 \quad (3)$$

Where S_s is the number of seed germinated in sample, S_c is the number seed germinated in control, R_s is the average root length in sample and R_c is the average root length in control.

Root and shoot length

Root length was taken from the point below the hypocotyls to the end of the tip of the root. Shoot length was measured from the base of the root-hypocotyl transission zone up to the base of the cotyledons. The root and shoot length was measured with the help of a thread and scale.

Seedling vigor index

The seedling vigor index was determined by using the formula.

Seedling vigor index = Average root length in cms + Average shoot length in cms × Germination percentage.

RESULTS AND DISCUSSIONS

X-ray diffraction (XRD) analysis (Figure 1).

The XRD pattern of the MgO sample calcined at 400°C for 2hrs is presented in Figure 1. All the peaks in Figure 1 corresponding be indexed to cubic MgO crystallites with the lattice parameter $a=0.421$ nm using the standard values of JCPDS 45-946. Peaks were absorbed at 36°, 42°, 62°, 74° and 78° along with miller indices values (1 1 1), (2 0 0), (2 2 0), (3 1 1) and (2 2 2), respectively. No peak arising from an impurity was observed in Figure 1. The average particle size in the calcined MgO nanoparticles was estimated by the Debye-Scherrer equation (Dinesh, 2012).

$$D = \frac{k\lambda}{\beta \cos \theta} \quad (4)$$

where D is the crystal size, k is the shape factor, which usually takes a value of about 0.9, λ is the wavelength of X-ray source used, β is the full width at half-maximum (FWHM), and θ is the Bragg diffraction angle. The average particle size of MgO calcined at 400°C was measured to be 22 nm.

FTIR analysis

From Figure 2 displays the FTIR curve of MgO NPs. The absorption bands in the range of 3418.6 cm⁻¹ are due to the stretching mode of -OH vibration. The absorption band at 1636.8 cm⁻¹ is due to bending vibration mode of physisorbed water. The intense peaks at 1458.2 cm⁻¹ are associated with vibrational mode of H⁻ ion bonded to Mg²⁺ on different co-ordination sites. The bands in between 649.5-561.1 cm⁻¹ are due to MgO vibrations.

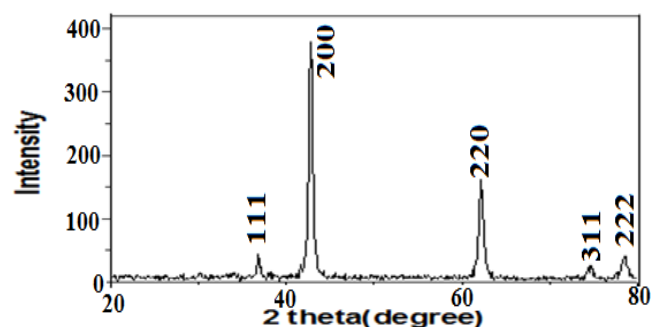


Figure 1: XRD pattern of MgO nanoparticles.

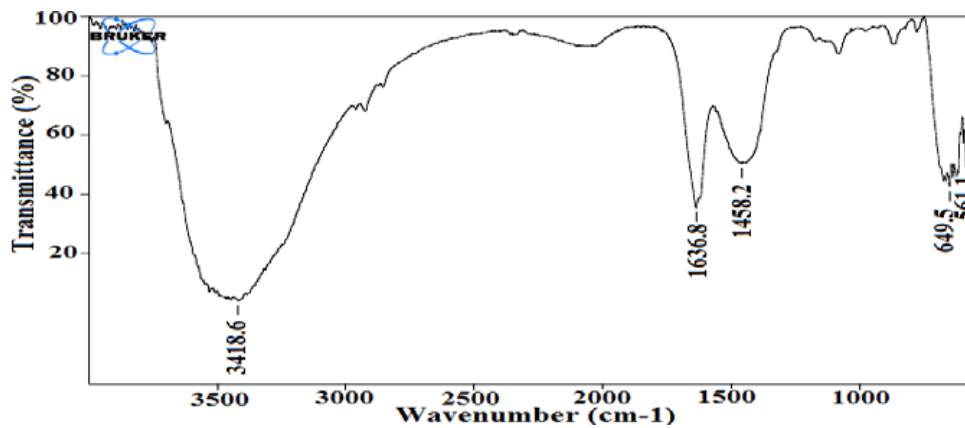


Figure 2: FTIR spectra of MgO nanoparticles.

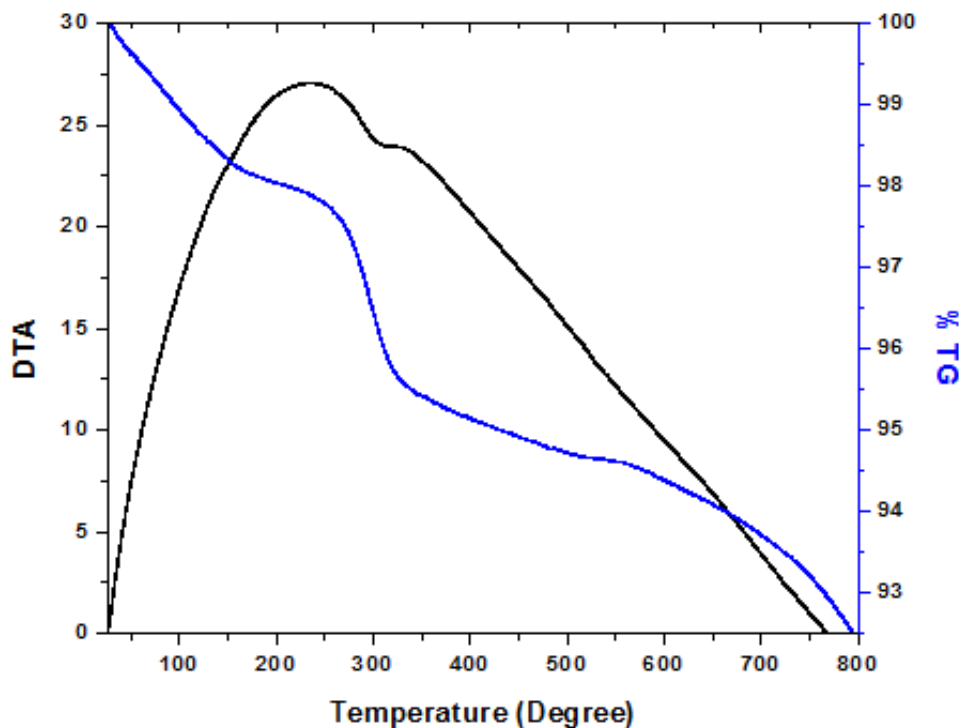


Figure 3: TG/TDA curve of MgO nanoparticles.

TGA-DTA analysis

Thermal properties of the MgO nanoparticles were observed by using TGA-DTA. In this thermo gravimetric and differential thermal analyser were analysed with the function of temperature. The weight loss of the material was calculated from TG curve. The analysis was observed from room temperature to 800°C, which is shown in Figure 3. Below 100°C the weight loss was observed due to water evaporation. After 100°C to 400°C the weight loss occurred due to the evaporation of inorganic material in the sample. Then the weight loss was happened due to the evaporation of surface unreacted organic and other materials of the sample. The total weight loss was calculated as 6.5% from room temperature to 800°C. This information was supported by DTA curve.

Particle Analyzer (Figure 4)

The average particle size was obtained by Particle Size Analyzer. The material was dispersed completely

in distilled water using ultra-sonicator. Below Figure 3 represents the histograms of the nanoparticles. The average particle size was obtained 40 nm. These results were supported to XRD average crystallite size.

SEM analysis (Figure 5)

The analysis of the scanning electron microscopy (SEM) images predicts the formation and the morphology of stable MgO nanoparticles obtained from the current green approach. The MgO NPs are mainly uniform agglomeration with the average range of particle size distribution is 2 μm (Figures: 6-10).

Germination percentage, RSG, RRG, GI, SVI, Biomass, fresh length and dry weight accumulation

The present study clearly indicates that MgO nanoparticles could be synthesized by a simple aqueous biogenic method using pure aqueous route resulting in primary particle sizes of 22 nm. In our current experiment, application of

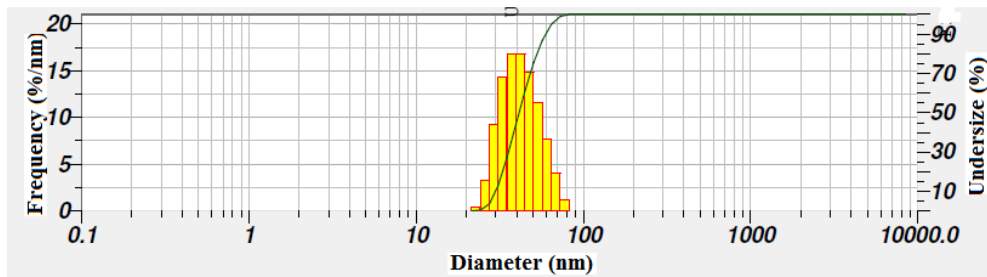


Figure 4: PSA analysis of MgO nanoparticles.

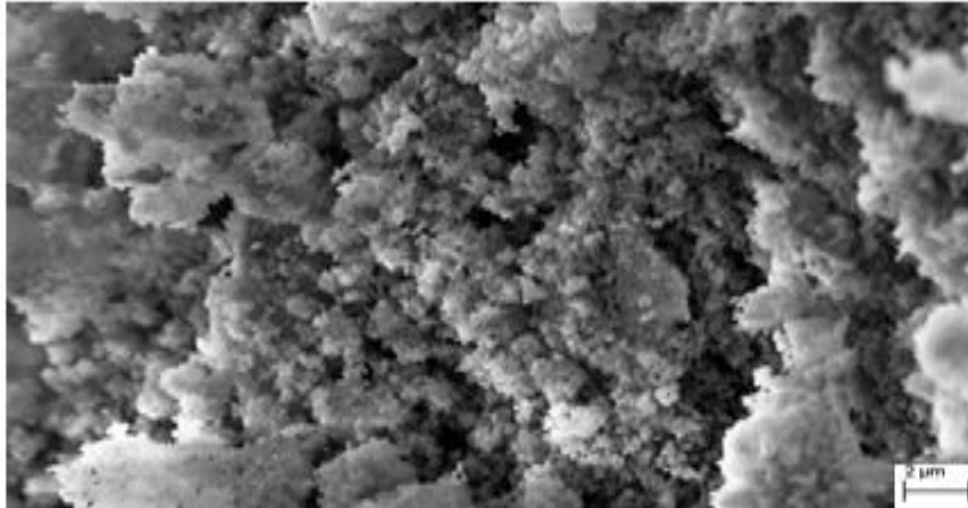


Figure 5: SEM analysis of MgO nanoparticles.



Figure 6: Germinated maize plant.

MgO stimulated the seed germination of maize. However, this response was dependent on the concentration of applied MgO on maize seed germination. In maize plant, results showed that the highest and the lowest GP (95% and 80%), were obtained in 100 mg concentration of nano-sized MgO and control, respectively (Ma, 2010). Our findings possibly revealed the use of nano-MgO (15-25 nm in diameter) increased the seed germination parameters of maize seeds. Results of germination test on plants indicated that the final GP was significantly affected by the employed treatment, however, increasing the concentration of nanosized MgO up to 150 mg caused an increase in seed germination and after that it declined. However, the maximum seedling SVI (1440) was observed in concentration (100 mg).

The vigor index of maize varied from 920 to 1440 in 12 hrs seed soaking period. Among the treatments, the highest mean vigor index value of 1520 was observed in 100 mg of MgO nanoparticles (V. Shah and I). The lowest mean vigor index value of 920 was recorded in control. The interaction between seed soaking periods and treatments were found significant.

The calculation carry our for fresh biomass analysis, before plant harvested after plant harvested. The whole plant along with leaves, shoot and root fresh weight was measured. For dry weight, the plant were dried in oven at 80°C weight was recorded. Biologically synthesized MgO nanoparticles effect on maize biomass when increase the concentrations increase the biomass of the maize plant (Zhu, 2008; Kurepa, 2010; Saha, 1990; Lu, 2002). The

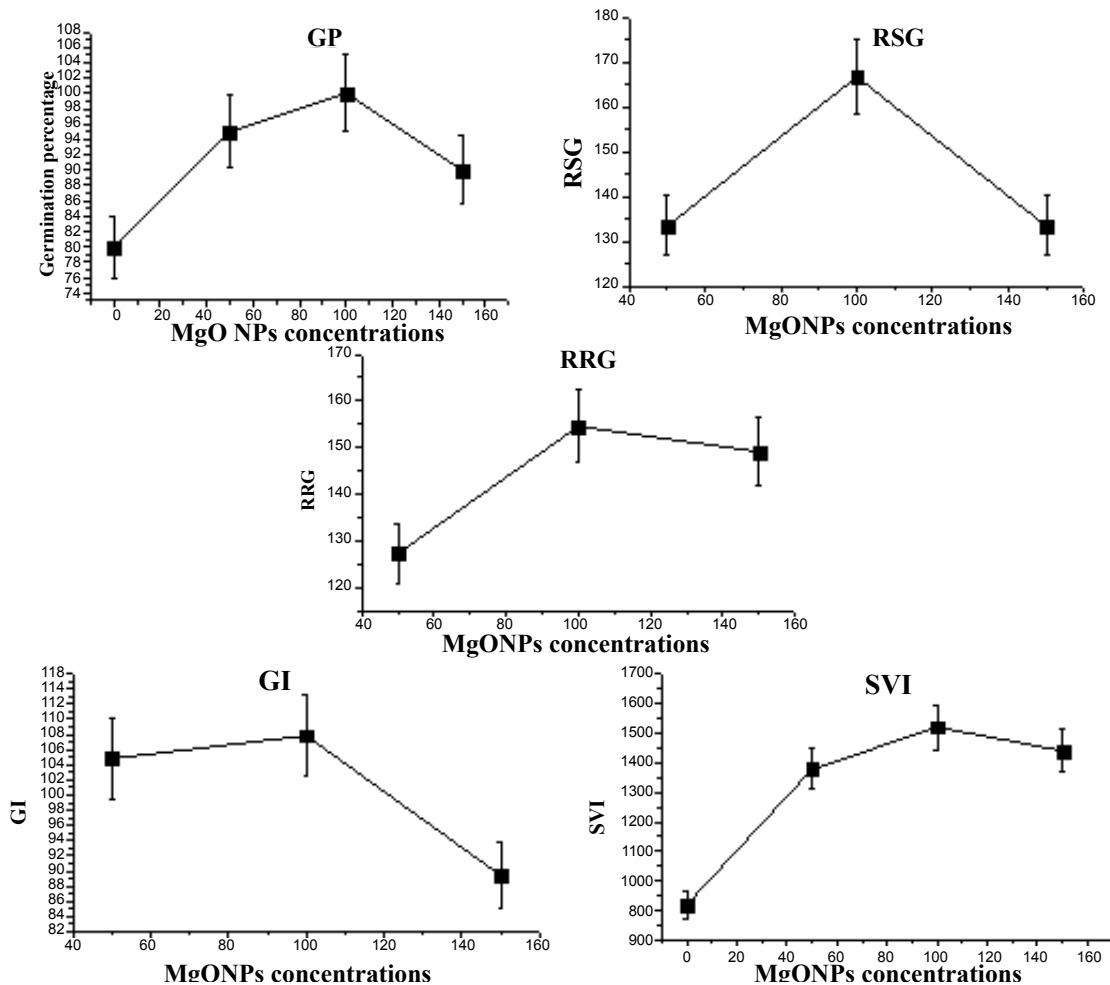


Figure 7: Effect of MgO NPs on growth parameters [X-axis MgO concentration 0.0, 50, 100 and 150 mg.L⁻¹, Y-axis GP, RSG, RRG, GI and SVI percentages].

biogenic MgO nanoparticles effect on biomass production of the maize plants.

The root length of maize varied from 5.5 to 7.3 cm for 12 hrs seed soaking period of maize. Among the treatments, the highest root length of 7.9 cm was recorded in nano MgO suspension-100 mg, which was significantly different from other treatments and control, whereas the lowest mean root length of 5.5 cm was recorded in control (Lee, 2008). The interaction effect depends on both soaking in periods and treatments of in nanoparticles. The shoot length of maize ranged from 7.2 to 9 cm in 12 h seed soaking period. Among the treatments, recorded the highest shoot length of 9.4 cm was recorded in nano MgO suspension - 100 mg. The lowest shoot length of 7.2 cm was recorded in control (Mahajan, 2011). The interaction effect depends on both soaking periods and treatments of in nanoparticles. Dry weight of a plant generally determines its growth and vigor. Dry weight accumulation after 20 days was treated with MgO nanoparticles. (Vashisth, 2010) Major part of incorporated MgO NPs had been utilized subsequently by the plant tissues for their metabolic processes (Yang, 2005). From this result it may be also conclude that as major part of the nano- MgO is utilized by the plants, the risk of bioaccumulation as well as chance

of toxicity in higher trophic level is reduced (Racuciu, 2007; Khot, 2012). This result is of great importance from agricultural perspective as we can apply this technique for increasing germination rate and vigor of crop plants.

MgO NPs effect on chlorophyll content in maize plant

Study the chlorophyll content in maize plant at 20 days of crop age. Effect on chlorophyll a, chlorophyll b, carotenoids, chlorophyll a/b and total chlorophyll content exposed to different concentration of MgO nanoparticle was observed in maize plants (Figure 10). The chlorophyll content of maize crop plants was tolerant by MgO nanoparticle concentrations therefore chlorophyll production was affected till 20 days. Exposure to 50, 100 and 150 mg.L⁻¹ of MgO nanoparticles reported significant on total chlorophyll content when compare to control after 20 days of treatment. It may be the MgO nanoparticles of 22 nm taken up by plants which were mostly in intracellular spaces could be transported inside plant cells through plasmodesmata of root cells (Ma, 2010). The MgO nanoparticles were then pass through shoots and then accumulated on leaves which caused adverse effect on total chlorophyll content of test plants. The reported that chlorophyll content of maize plants was found to be increased by low concentration

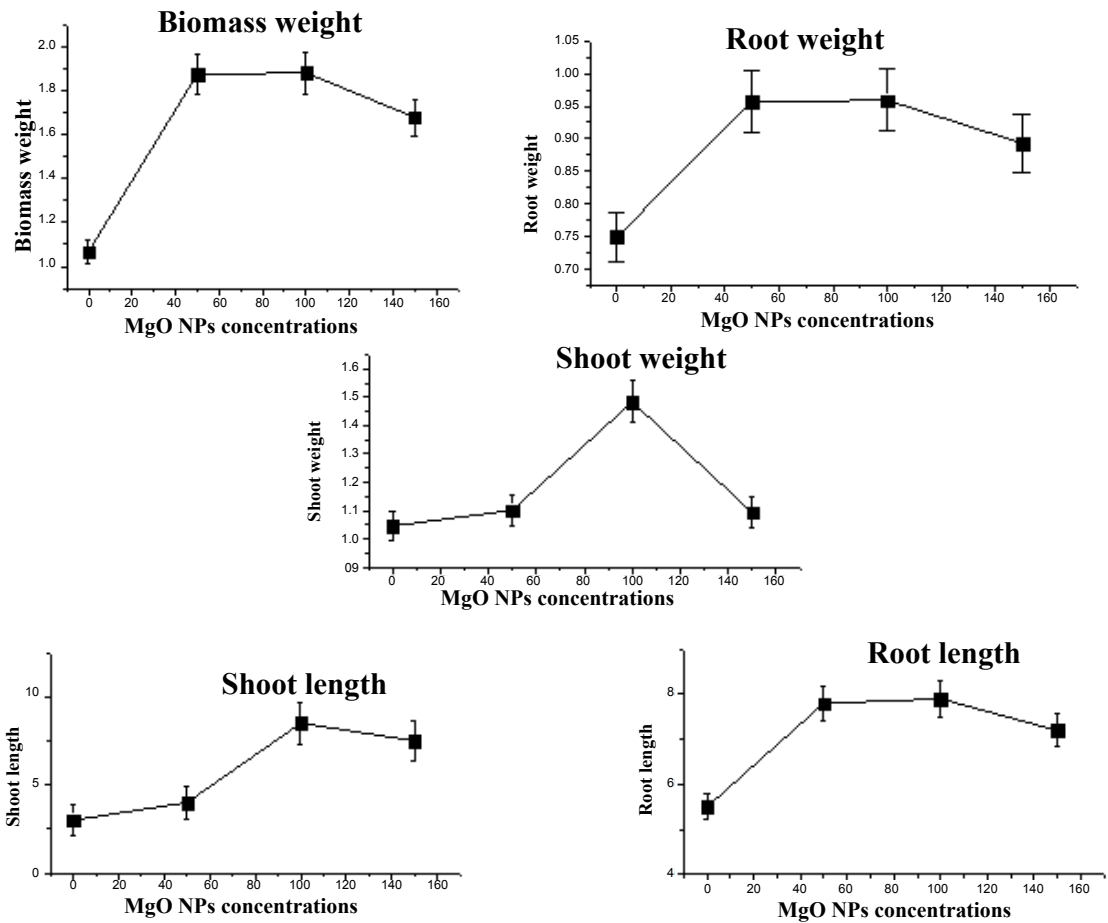


Figure 8: Effect of MgO NPs on fresh biomass weight and length [X-axis MgO concentration 0.0, 50, 100 and 150 mg.L⁻¹, Y-axis weight (gms), length (cms)].

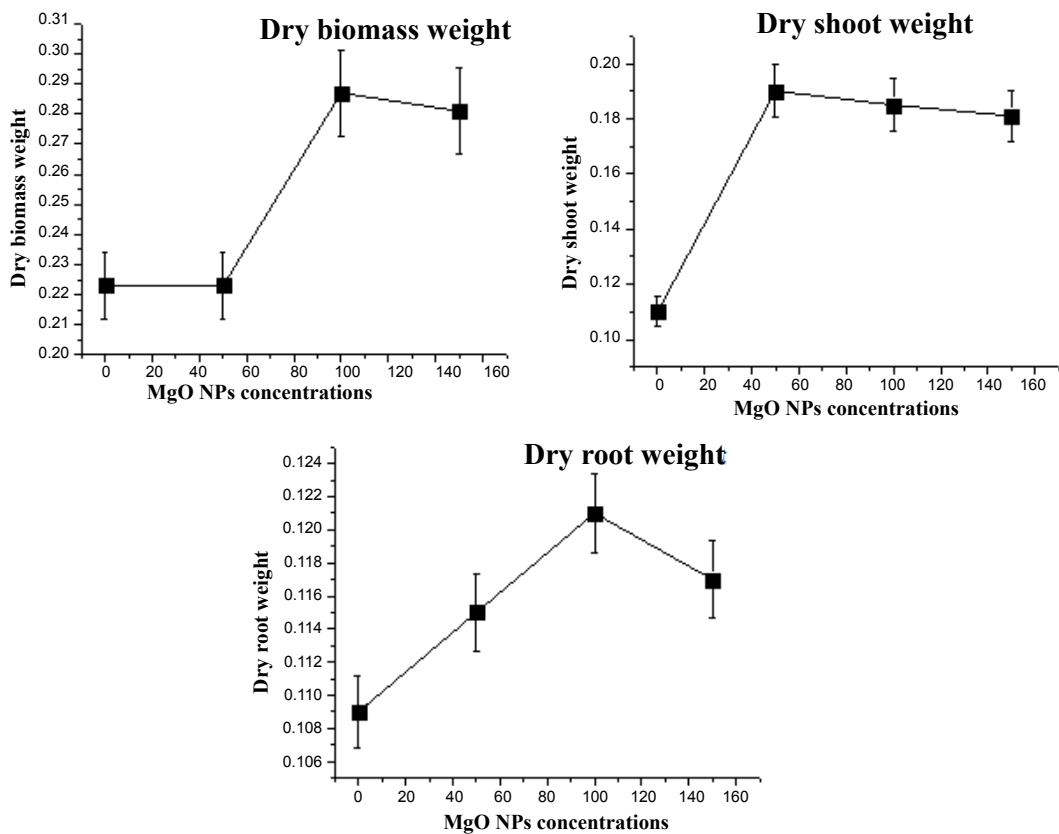


Figure 9: Effect of MgO NPs on Dry weight [X-axis MgO concentration 0.0, 50, 100 and 150 mg.L⁻¹, Y-axis dry weight (gms)].

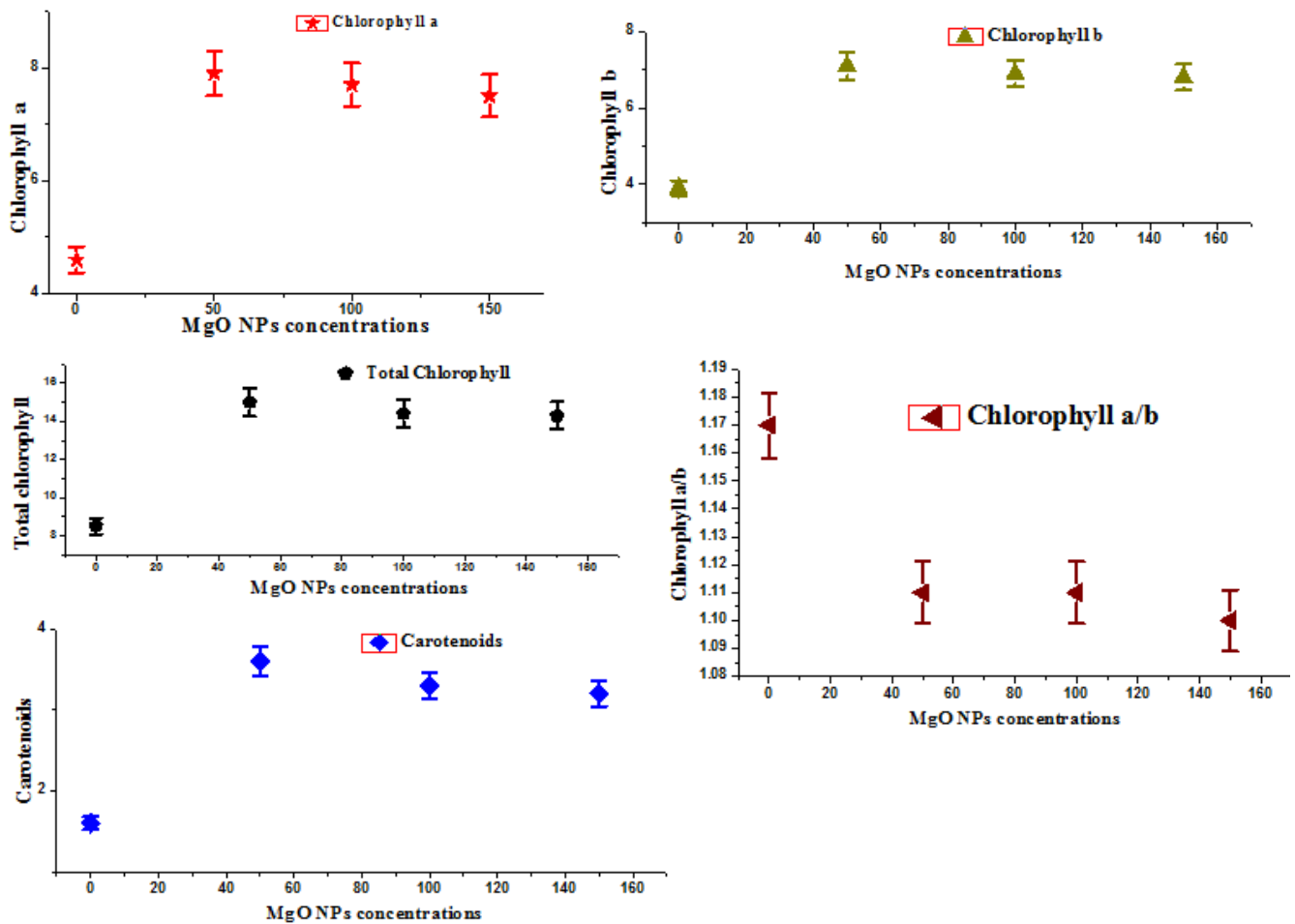


Figure 10: Effect of MgO NPs on Chlorophyll [(X-axis MgO concentration 0.0, 50, 100 and 150 mg.L⁻¹, Y- axis chlorophyll)].

(50 mg.L⁻¹) while it was found to be inhibited by higher concentrations of MgO nanoparticle (Zhu, 2010). Figure 10 shows the effect on chlorophyll content of test plants by MgO nanoparticle; decrease in chlorophyll content was observed in maize with increase in concentration of nanoparticle solution. It was reported that increase in Hill reactions and activity on chloroplasts in plant by nano-TiO₂ resulted in an acceleration of Fe Cy reduction and oxygen evolution in *Spinacia oleracea* (Hong, 2005; Hong, 2005). Thus we can assume that MgO nanoparticles at higher concentration (50, 100 and 150 mg.L⁻¹) may directly affect the LHC II content on thylakoid membrane of selected test plants (Figure 11).

The maize plants were dried in oven (75°C) these dried plant material then grounded fine powder for FTIR analysis. It is clear from the spectra that the bonds appeared in sharp stretching bonds presence 100 mg.L⁻¹ and 150 mg.L⁻¹ concentration MgO NPs treated maize plants whereas compare to 50 mg.L⁻¹ and control. The band at 850 to 1190 cm⁻¹ associated with C=O stretching vibration indicating the possible involvement of C=O within the plant body and indicate the carbohydrate formation. The observed that the band areas at 1650 to 1750 cm⁻¹ amide region. The sharp stretching bond presence in only 100 mg.L⁻¹ concentration treated maize plant whereas compare to other treatments

and control. The sharp stretching bond appeared at 3000 to 3500 cm⁻¹ (in 100 mg.L⁻¹ concentration treated maize plant) due to absorbed water and lipids content. From this result we can also conclude that as major part of the nano MgO is utilized by the maize plants (Figure 12).

In this study the nanoparticles is present in a plant cell is analysis by SEM. the maize plant samples of the roots were placed in 3.5% glutaraldehyde solution. This may have led to more accumulation of MgO nanoparticles in the roots and then transport to shoots (stem and leaves). In this experiment uptake of MgO nanoparticles at different concentrations of 50 mg.L⁻¹, 100 mg.L⁻¹ and 150 mg.L⁻¹ was found to be significant, with few white dots appearing root surface of the maize plants.

CONCLUSION

Magnesium oxide nanoparticles were successfully produced using bio-combustion method. The XRD and FTIR analysis confirmed the complete transformation of MgO nanoparticles after calcinations. In this study we have observed beneficial role of nano- MgO NPs in seed germination and plant growth regulation in maize. The possible reason for such beneficial role is the increase in activity of growth hormones. The nanoparticles size play important role in the behavior, reactivity and effect

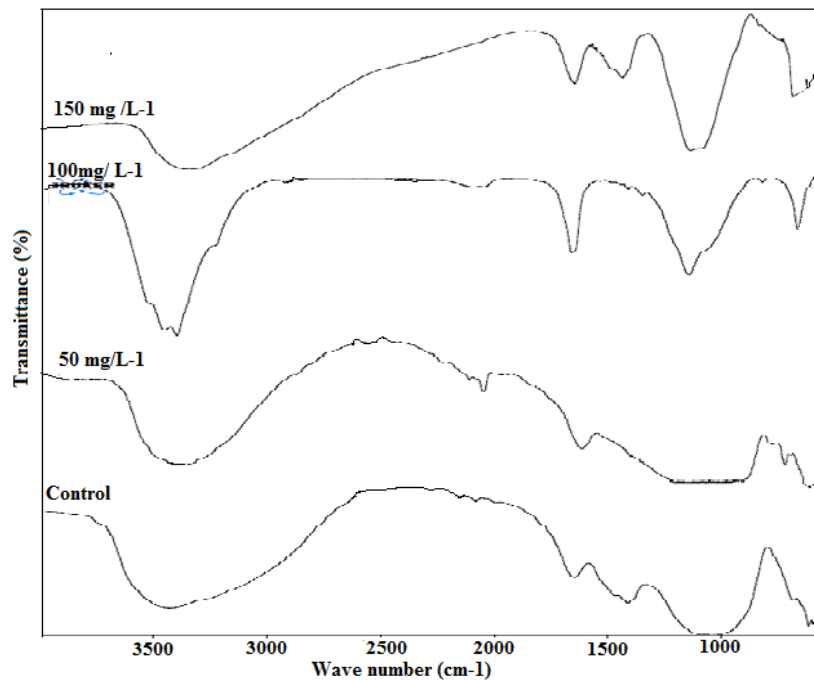


Figure 11: FTIR spectra of maize plant treated with control, 50 mg.L⁻¹, 100 mg.L⁻¹ and 150 mg.L⁻¹.

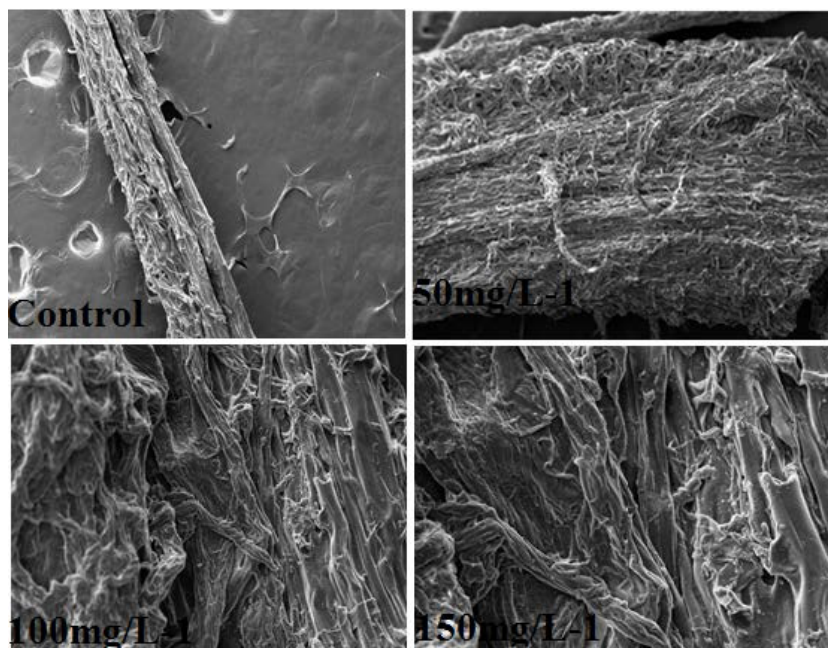


Figure 12: SEM images of the topography of the root region of the germinated maize seedling grown in soil

of nanoparticles was observed on growth parameters of maize. Overall, the present study demonstrates possible adverse effect of metal oxide nanomaterials on plants. MgO NPs penetrates easily inside the plant cells and causes effects on plant biomass and chlorophyll content. Results clearly demonstrate the greater improvement in biomass shoot-root growth and photosynthetic pigment (chlorophyll) by the application of biologically synthesized MgO nanoparticle at 50 mg.L⁻¹ and 100 mg.L⁻¹ concentrations on 20 days plants.

ACKNOWLEDGEMENT

My special thanks to University Grants Commission for providing the financial support.

REFERENCES

- Adams, L.K., Lyon, D.Y. and Alvarez, P.J.J., (2006). Comparative eco-toxicity of nanoscale TiO₂, SiO₂, and ZnO water suspensions. *Water. Res*, 40: 3527²-3532².
- Aoshima, H., Kokubo, K., Shirakawa, S., Ito, M., Yamana, S. and Oshima, T., (2009). Antimicrobial activity of fullerenes and their hydroxylated derivatives. *Biocontrol Sci*, 14: 69 -72.
- Aruoja, V., Dubourguier, H.C., Kasemets, K. and Kahru, K., (2009). Toxicity of nanoparticles of CuO, ZnO and TiO₂ to microalgae *Pseudokirchneriella subcapitata*. *Sci Total Environ*, 407: 1461 -1468.

- Brar, S.K., Verma, M., Tyagi, T. and Surampalli, R.Y., (2010). Engineered nanoparticles in wastewater and wastewater sludge -Evidence and impacts. *Waste Management*, 30: 504 -520.
- Canas, J.E., Long, M., Nations, S., Vadan, R., Dai, L., Luo, M., Ambikapathi, R., Lee, E.H. and Olszyk, D., (2008). Effects of functionalized and non-functionalized single-walled carbon nanotubes on root elongation of select crop species. *Environ Toxicol Chem*, 27: 1922-1931.
- Colvin, V.L., (2003). The potential environmental impact of engineered nanomaterials. *Nat Biotechnol*, 21: 1166-1170.
- DeRosa, Me., Monreal, C., Schnitzer, M., Walsh, R. and Sultan Y., (2010). Nanotechnology in fertilizers. *Nat Nanotechnol*, 5: 91.
- Dinesh, R., Anandaraj, M., Srinivasan, V. and Hamza, S., (2012). Engineered nanoparticles in the soil and their potential implications to microbial activity. *Geoderma*, pp: 173-174, 19-27.
- Hong, F., Zhou, J., Liu, C., Yang, F., Wu, C., Zheng, L. and Yang, P., (2005). Effect of nano-TiO₂ on photochemical reaction of chloroplasts of spinach. *Biol. Trace Elem. Res.*, 105: 269-279.
- Hong, F., Yang, F., Liu, C., Gao, Q., Wan, Z., Gu, F., Wu, C., Ma, Z., Zhou, J. and Yang, P., (2005). Influence of nano-TiO₂ on the chloroplast aging of spinach under light. *Biological Trace Element Research*, 104: 249-260.
- Kurepa, J., Paunesku, T., Vogt, P., Arora, H., Rabatic, R.M., Lu, J.J., Wanzler, M.B., G.E., Woloschak, and Smalle, J.A., (2010). Uptake and distribution of ultrasml anatase TiO₂ alizarin red S nanoconjugates in arabidopsis thaliana. *Nano Lett*, 10: 2296.
- Khot, L.R., Sankaran, S., Mari, Maja, J., Ehsani, R. and Schuster, E.W., (2012). Application of nanomaterials in agriculture and crop protection: a review, *Crop Protection*, 35: 64-70.
- Lu, C.M., Zhang, C.Y., Wen, J.Q., Wu, G.R. and Tao, M., (2002). Research of the effect of nanomaterials on germination and growth enhancement of Glycine Max and its mechanism. *Soybean Science*, 21: 168-171.
- Lee, W.M., An, Y.J., Yoon, H. and Kweon, H.S., (2008). Toxicity and bioavailability of copper nanoparticles to the terrestrial plants Mung Bean (*Phaseolus radiatus*) and Wheat (*Triticum aestivum*): Plant agar test for water-insoluble nanoparticles. *Environ. Toxicol. Chem*, 27: 1915-1921.
- Mahajan, P., Dhoke, S.K. and Khanna, A.S., (2011). Effect of Nano-ZnO Particle Suspension on Growth of Mung (*Vigna radiata*) and Gram (*Cicer arietinum*) Seedlings Using Plant Agar Method, *Journal of Nanotechnology*, 7.
- Ma, X, Lee, J.G., Deng, Y. and Kolmakov, A., (2010). Interactions between engineered nanoparticles (ENPs) and plants: Phytotoxicity, uptake and accumulation, *Science of the Total Environment*, 408: 3053-3061.
- Ma, Y.H., Kuang, L.L., He, X., Bai, W., Ding, Y.Y., Zhang, Z.Y., Zhao, Y.L. and Chai, Z.F., (2010). Effects of rare earth oxide nanoparticles on root elongation of plants. *Chemosphere* 78: 273.
- Racuciu, M. and Creanga, D.E., (2007). TMA-OH Coated magnetic nanoparticles internalized in vegetal tissue. *Rom. Journ. Phys.*, 52: 395-402.
- Shah, V. and Belozerova, I., (2009). Influence of metal nanoparticles on the soil microbial community and germination of Lettuce Seeds. *Water Air Soil. Poll*, 197: 143.
- Saha, R., Mandal, A.K. and Basu, R.N., (1990). Physiology of seed invigoration treatments in Soybean (*Glycine max L.*). *Seed Science and Technology*, Zürich, 18: 269-276.
- Vashisth, A. and Nagarajan, S., (2010). Effect on germination and early growth characteristics in sunflower (*Helianthus annuus*) seeds exposed to static magnetic field, *J Plant Physiology*, 167: 149-156.
- Yang, L. and Watts, D.J., (2005). Particle surface characteristics may play an important role in phytotoxicity of alumina nanoparticles, *Toxicological Letters*, 158: 122-132.
- Zhu, H., Han, J., Xiao, J.Q. and Jin, Y., (2008). Uptake, translocation, and accumulation of manufactured iron oxide nanoparticles by Pumpkin plants. *Journal of Environmental Monitoring*, 10: 713-717.